Tellus (1989), *41A*, 222–245

An observational case study of a continental mesoscale vortex

By ERNEST M. AGEE and JAMES J. LIDRBAUCH[1], *Department of Earth and Atmospheric Sciences, Purdue University, West Lafayette, Indiana 47907, USA*

(Manuscript received 9 February 1987; in final form 19 July 1988)

ABSTRACT

An observational case study of a continental mesoscale vortex embedded in a polar air stream has been conducted, with emphasis on observed vortex features and their possible relationship to the polar-low phenomena and accompanying synoptic scale features at the 850 mb, 700 mb and 500 mb levels. The path of this 14–16 December 1983 event (determined from GOES satellite imagery) was over the relatively data-rich region of the midwestern United States, with the mesoscale vortex rotating cyclonically around and to the south of an occluded synoptic-scale surface low pressure system (and 500 mb low). This case study exhibited features common to the polar low with its convective cloud mass, although a distinct surface signature never developed. The mesoscale vortex formed and remained within a strong cyclonic shear region (4×10^{-5} s^{-1}) at the 850 mb level, but was supported by the evolution of a baroclinic pattern as well. Spatial and temporal cross-sections (both horizontal and vertical) revealed a weak low-level warm core capped by a strong cold dome, most pronounced at the 700 mb level and distinctly separate from the synoptic scale low in the surface map and 500 mb height field. This low static stability mesoscale system occurred entirely beneath the 500 mb level with cloud tops near 600 mb, and was associated with a weakly defined 600 km wave at the 700 mb level. The pure CISK model results for wavelength growth by Bratseth and the combined moist baroclinicity and CISK studies by Sardie and Warner correspond best to this continental event. It is suggested that both barotropic and baroclinic instability mechanisms (combined with CISK) can exist cooperatively in support of the development and maintenance of both continental and maritime polar low events.

1. Introduction

The polar low phenomenon has received increasing attention over the past two decades. It was traditionally considered as a thermal instability in a polar air mass flowing over a warm sea, because of the strong argument for thermal enhancement by the intense sensible and latent heat fluxes from the open water. Harrold and Browning (1969) first questioned this concept by showing considerable low-level baroclinicity associated with a number of polar low cases. Mansfield (1974) used a model of limited vertical extent to show that the small wavelength could be due to the shallowness of the disturbance. In addition, he showed that surface heating and friction can contribute adversely to polar low development. Duncan (1977) found that weak static stabilities at low levels reduce the wavelength of maximum growth rate to polar low dimensions. Rasmussen (1979) rejected the theory of baroclinicity for this phenomenon and proposed that the polar low is an example of an extratropical CISK phenomenon by showing that small unstable CISK disturbances can develop in conditions similar to those that surround developing polar lows. Reed (1979) introduced the comma cloud as the North Pacific version of the polar low and found deep baroclinicity and conditional instability through a substantial portion of the troposphere.

[1] Present affiliation: *The Analytic Sciences Corporation, Reading, MA 01867, USA.*

Also, the necessary condition for barotropic instability is usually satisfied for comma cloud polar lows (Reed, 1979; Harrold and Browning, 1969). Although the jet stream would have to be unusually strong and narrow for barotropic instabilty to be the sole mechanism producing disturbances on a scale as small as the polar low (Reed, 1979; Mullen, 1979; Nitta and Yanai, 1969), barotropic instability cannot be ruled out as a possible important additional influence on the formation of polar lows (Reed, 1979). Reed attributed the small wavelength of the polar low to the effects of small static stabilities at low levels (see Gall, 1976; Staley and Gall, 1977; Duncan, 1977) and suggested that the disagreements with the baroclinic theory might not hold up if the baroclinic models used an already perturbed basic state instead of the more common zonal basic state.

Mullen (1979) defined statistically the basic zonal state in which Pacific comma clouds form and develop. He proposed that these disturbances are primarily baroclinic but the latent heat release (CISK) and non-linear processes could be responsible for features of the observed structure not explained by linear baroclinic theory. Rasmussen (1981) showed that at least some polar lows are of a more convective type and are different from the comma cloud polar lows associated with secondary positive vorticity centers aloft.

The inclusion of baroclinicity as one of the major forcing mechanisms has provided a mechanism by which a mesoscale vortex, similar to the polar low, can form over land. Reed (1979) and Mullen (1982) cite examples of mesoscale cyclones in polar air streams over the North American continent that are very similar to those which occur over the oceans. These have occurred in air masses of negligible moisture content so CISK probably did not play a major role in the development. Rasmussen (1985) disagrees with the concept of continental polar lows and states, "polar low developments have never been observed over land, and on the contrary, they almost invariably decay rapidly after landfall," but he qualifies his statement, noting a dependence upon one's definition of polar low. Locatelli et al. (1982) studied the mesoscale structure of several examples of Pacific comma clouds and noted that "there is some evidence that two types of vortices may exist", the first type being the comma cloud variety and the second type being a disturbance that develops farther back in the polar air and is more convective than the first.

The comma cloud variety is found in both the Pacific and the Atlantic (Rasmussen, 1985) and is the most common manifestation of the polar low in the Pacific (Reed, 1979; Mullen, 1979; Locatelli et al., 1982). The spiral-form variety is rare in the Pacific, though it has been noted occasionally in the Gulf of Alaska region (Businger, 1987). It is generally found in the North Atlantic region, especially in the Barents Sea, Norwegian Sea and south and west of Iceland (Rasmussen, 1985). Recent case studies of polar low events in the Gulf of Alaska and the Bering Sea by Businger (1987) show many similarities to those that occur in the Norwegian and Barents Seas (also, see Businger (1985)).

The difference between the comma cloud and the spiral-form polar low seems to be the degree to which convection dominates the development of the disturbance (Locatelli et al., 1982; Sardie and Warner, 1983; Rasmussen, 1985). Thus, comma clouds seem to be less convective and dominated by baroclinic processes, while spiral-form polar lows are characterized by a more convective cloud mass, though shallow baroclinicity may also be present.

Carleton (1985b) used a satellite cloud image classification system (see Carleton, 1985a) to present climatological aspects of both the polar low and the instant occlusion. He reaffirmed the tendency for comma clouds to occur over the Pacific region and spiral-form polar lows to occur over the North Atlantic, attributing the latter at least partly to the effect of the Arctic sea–ice boundary. The climatology of well-developed North Atlantic polar lows has been presented by Businger (1985), based largely on analyses at the 500 mb level. Additional climatology on polar low events in the North Pacific have been given by Businger (1987), drawing particular attention to features at the 500 mb level for polar low formation.

This paper will present an analysis of a continental mesoscale vortex event, which occurred over the midwestern United States during 14–16 December 1983. Similarities and differences of this event to the polar low phenomenon will be discussed, based on both observational and theoretical model results. The vortex studied here was first observed in the polar air stream over eastern Nebraska and was moving to the southeast. It later turned northeastward, where it underwent increased development into a spiral-form cloud pattern evident in GOES satellite images. It was only weakly discernible in the surface weather map throughout its lifetime, but it did produce a persistent area of heavy snow showers.

2. Models, data and analysis techniques

To test which instability mechanism dominates, baroclinicity or CISK, Sardie and Warner (1983) used a 3-layer quasi-geostrophic model to study the relative effects of baroclinicity and latent heating. They concluded that Pacific polar lows (comma clouds) could be explained by moist baroclinicity while a combination of moist baroclinicity and CISK was required to explain the development of Atlantic polar lows. Sardie and Warner (1985) used the Penn State/NCAR mesoscale model to analyze a Pacific and an Atlantic polar low, and found combined moist baroclinicity and CISK essential for cyclogenesis.

Bratseth (1985) pointed to a limitation in the modeling of the horizontal heating distribution in previous studies (e.g., Rasmussen, 1979; Sardie and Warner, 1983) and presented a more simple model of the CISK concept which suggests that CISK growth rates in the two above-mentioned papers are likely too high. This indicates that CISK in polar air masses is possible if the heating takes place in a shallow layer at low levels.

The Sardie and Warner (1983) model (SW) and the Bratseth (1985) model, along with a number of analysis techniques, were used to study this mesoscale vortex event. The three-layer, two-dimensional, quasi-geostrophic SW model, developed to study the relative importance of baroclinicity and CISK in polar-low events, was applied to compare the 14–16 December case study with the five Atlantic and two Pacific cases examined in the SW study. The analytical model developed by Bratseth (1985) was also applied to the 14–16 December case study data.

In addition to the model comparisons and calculations, several objective and hand-drawn analyses were derived to aid in the observational study of this case. The Purdue Regional Objective Analysis of the Mesoscale (PROAM) package was deployed to facilitate a more objective analysis of surface mesoscale features. Smith and Leslie (1982) provide a complete description of PROAM including some test results, and Smith et al. (1986) present an error analysis of PROAM. An upper air version of PROAM was also developed (PROAMU) by the authors to analyze the meteorological variables at each of the mandatory pressure levels. A third analysis package used was the Kinematic Analysis of the Mesoscale (KAM) package, based on the analysis method presented by Sheu and Agee (1977). KAM provides skew T–log p diagrams, calculates and plots vertical profiles of vorticity, divergence and vertical motion, as well as vertical cross-sections for a number of dynamic and thermodynamic variables in both space and time.

A number of data sources was used in this research, consisting of conventional surface and upper air data, GOES satellite and radar imagery, as well as special surface and upper air data collected in the vicinity of Lake Michigan. Routine hourly surface observations and 12-hourly rawinsonde reports were obtained for the stations depicted in Fig. 1. The special data sets were provided by Project LESS (Lake Effect Snow Studies) conducted in the vicinity of Lake Michigan during 1 December 1983 through 31 January 1984.

3. Case study results

3.1. *Synoptic discussion*

The 1200 GMT 14 December surface pressure analysis (Fig. 2a) shows four lows from the central Plains to New England, dominated by the occluded system over central Indiana with a central pressure of 995 mb. At this time, this low was also the dominant feature in the 850 mb height field (see Fig. 2b) and exhibited further tilt to the west with height such that the 500 mb low (5260 m) was centered over southeast Nebraska (see Fig. 3). The 500 mb map also shows an accompanying absolute vorticity maximum of 20×10^{-5} s^{-1}. It is noted that the occurrence and occlusion of the primary low over the Great Lakes region was in response to a short wave that entered the USA northwest coast at 0000 GMT

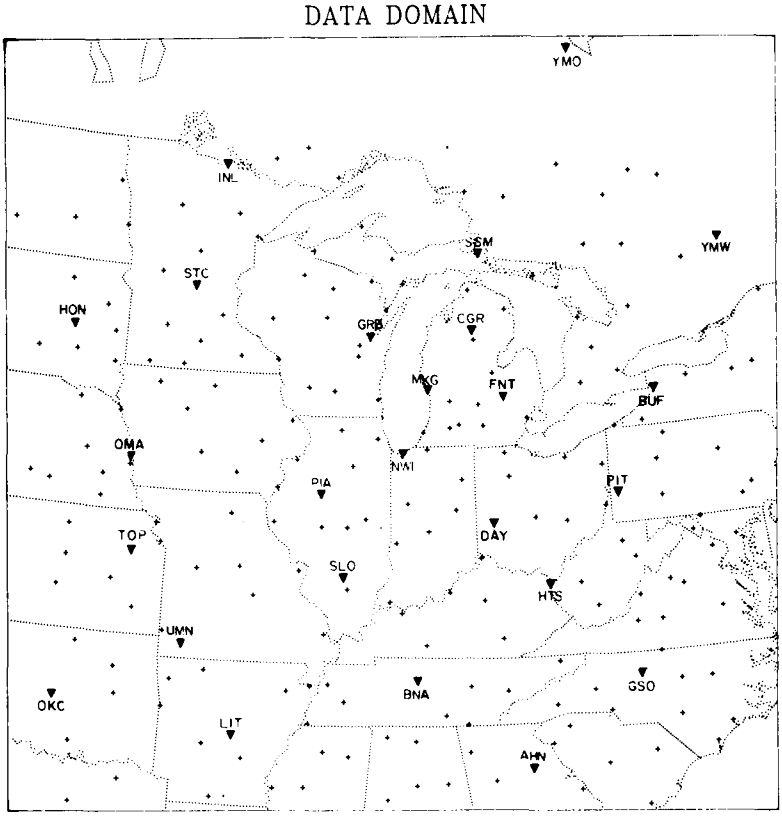

Fig. 1. Data network of routine surface (+) and upper air stations (▼), including special field program stations (NWI, MKG, CGR).

12 December. This wave moved to the center of the Mississippi Valley at 1200 GMT 14 December (see Fig. 2b), with strong wind shear between North Platte, Nebraska (LBF) and Omaha, Nebraska (OMA). It is suspected that this strong 850 mb cyclonic shear region (26 m s^{-1} to 10 m s^{-1}, giving a vorticity value of about 4×10^{-5} s^{-1}) was instrumental in the formation of a lower troposphere mesoscale vortex over eastern Nebraska, barely discernible in satellite imagery.

By 0000 GMT 15 December, the surface synoptic scale low had moved almost directly north from west-central Indiana to a position over central Lake Michigan, attaining a central pressure of 992 mb (see Fig. 4a). Fig. 4a–b shows the secondary cold front that moved out of the Northern Plains states, which trailed the mesoscale vortex into southern Illinois. In this and subsequent figures, the asterisk (*) locates the position of the mesoscale vortex, as determined from satellite imagery. The 500 mb low (5250 m) positioned in northern Missouri, subsequently moved to northern Michigan and weakened to 5270 m as an open wave (see Figs. 5a–b). Surface temperatures were in the -5°C to -10°C range through Kansas and Missouri. The 0030 GMT 15 December GOES IR satellite image (Fig. 6) shows an extensive cloud swirl with the surface low (L_1) over Wisconsin. The bright convective mesoscale cloud pattern over western Missouri identifies the mesoscale α vortex, noted by L_2.

The 1200 GMT 15 December 1983 surface analysis (Fig. 4b) shows little movement of the main low center L_1 with a 4 mb filling to a central pressure of 996 mb. The low is now

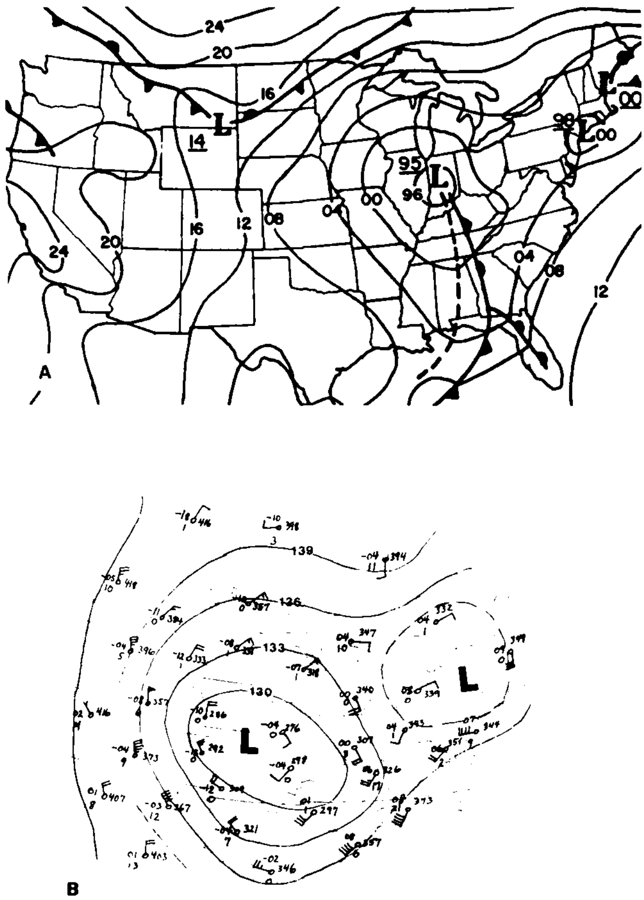

Fig. 2. (a) 1200 GMT 14 December 1983 surface analysis. (b) 1200 GMT 14 December 1983 850 mb analysis. Contours are labeled in decameters.

associated with a stationary front oriented generally southwest to northeast. The 1200 GMT GOES IR image (Fig. 7) shows a better developed cloud pattern associated with the mesoscale α vortex (now larger than initial formation), which was located over southeastern Illinois just southwest of Terre Haute, Indiana. Earlier images showed that the center of this mesoscale disturbance traveled almost directly over Salem, Illinois (SLO) at the time of the 1200 GMT sounding.

A number of GOES satellite images near 1200 GMT 15 December distinctly revealed the mesoscale vortex L_2. The 1030 GMT IR image (not presented) showed the comma-shaped cloud pattern in southern Illinois just prior to the passage of the polar low over Salem, Illinois. Fig. 8 reveals the structure of the vortex over central Indiana in the 1530 GMT visible satellite image. Note the clearing in the synoptic overcast induced by the vortex, which extended as far as northern Indiana. This mesoscale vortex is clearly not associated with the surface front, and is a distinct subsidiary vortex rotating around and to the south of the primary occluded system (at both the surface and 500 mb levels). The synoptic low L_1 is marked by the swirl in the cloud pattern just west of Lake Michigan and south of Green Bay, Wisconsin. Also, a small, intense snow shower (an S+ radar echo) was associated with

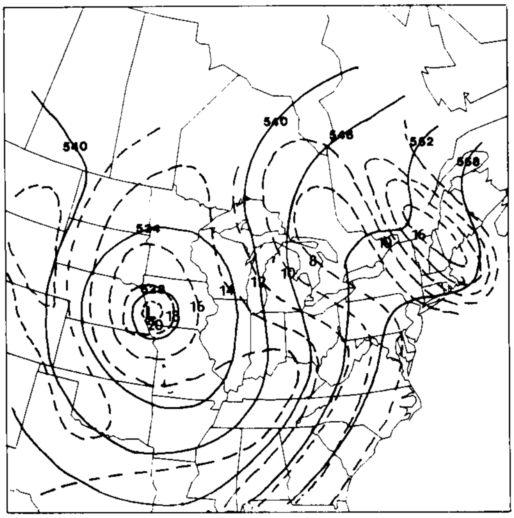

Fig. 3. 500 mb height field in decameters (solid line) and absolute vorticity analysis (10^{-5} s^{-1}) (dashed line) at 1200 GMT 14 December 1983.

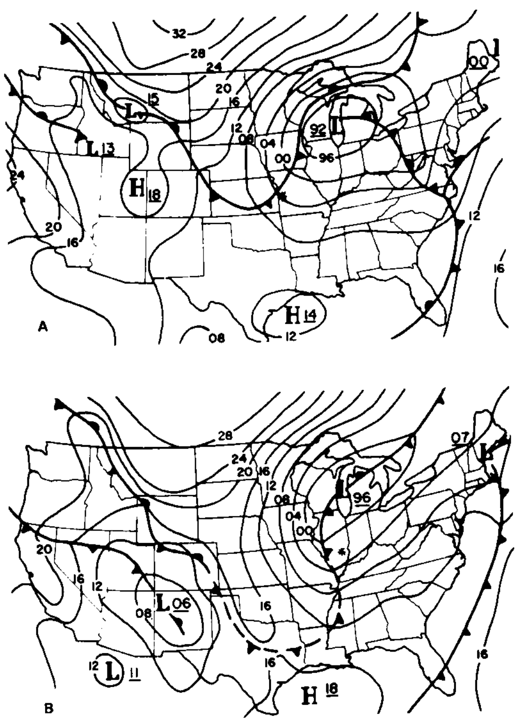

Fig. 4. (a) 0000 GMT 15 December surface analysis. In this and the following figures, the asterisk (*) denotes the position of the mesoscale vortex. (b) 1200 GMT 15 December surface analysis.

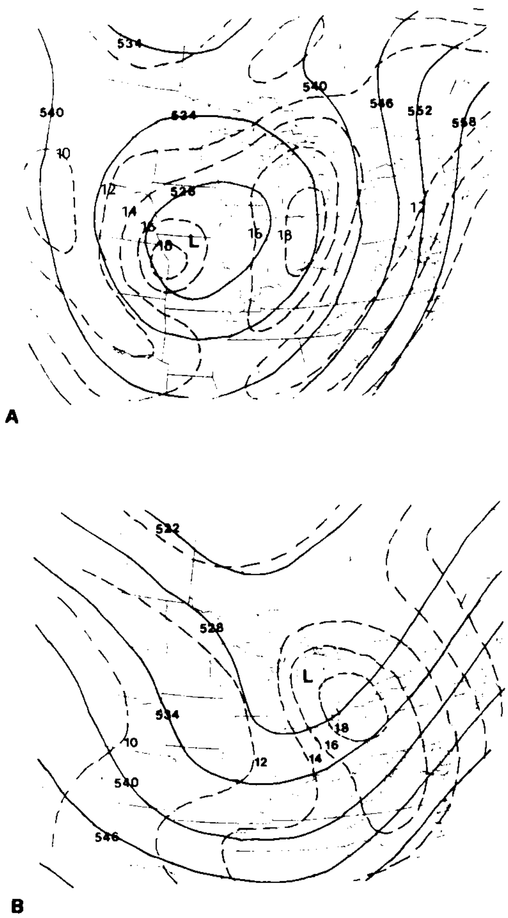

Fig. 5. (a) 500 mb height field in decameters (solid line) and absolute vorticity analysis in 10^{-5} s^{-1} units (dashed line) at 0000 GMT 15 December 1983. (b) Same as (a) except at 0000 GMT 16 December 1983.

the mesoscale low L_2, which traveled with the vortex system from 1200 GMT (near the Indiana–Illinois border) to about 1700 GMT (near the Indiana–Ohio border). The 1731 GMT visible image (Fig. 9) shows the mesoscale vortex L_2 in eastern Indiana, with indications of an eye-like structure and spiral feeder bands. And finally, the 2300 GMT IR image (Fig. 10) shows the mesoscale vortex L_2 just north of Lake Erie with the spiral structure still evident, even in the low resolution of the IR imagery. Two additional mesoscale disturbances appeared to the west (denoted by "X" in Fig. 10), but were even weaker than the case study presented here.

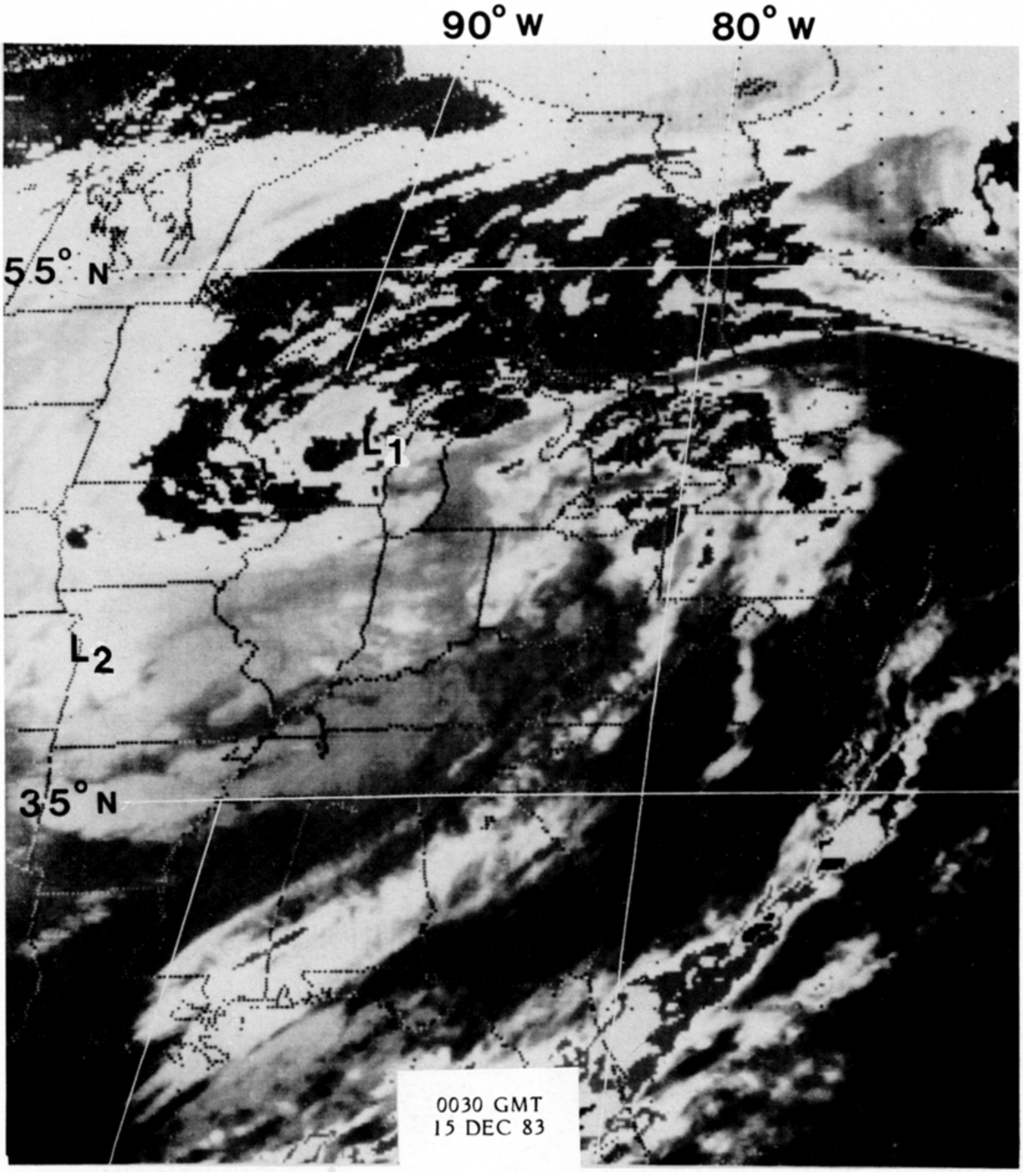

Fig. 6. GOES infrared satellite imagery at 0030 GMT 15 December 1983. L_1 identifies the location of the primary synoptic scale low over eastern Wisconsin. L_2 locates the mesoscale vortex event over western Missouri.

All mesoscale disturbances rotated cyclonically around the primary occluded system, now located over central Michigan.

By 0000 GMT 16 December 1983, the surface synoptic low had filled further (along with the 500 mb low) to 1003 mb, and had moved east to north-central Michigan (see Fig. 11a). The location of the mesoscale low is again identified with an asterisk (*). The weak secondary cold front extended south to central Indiana and a

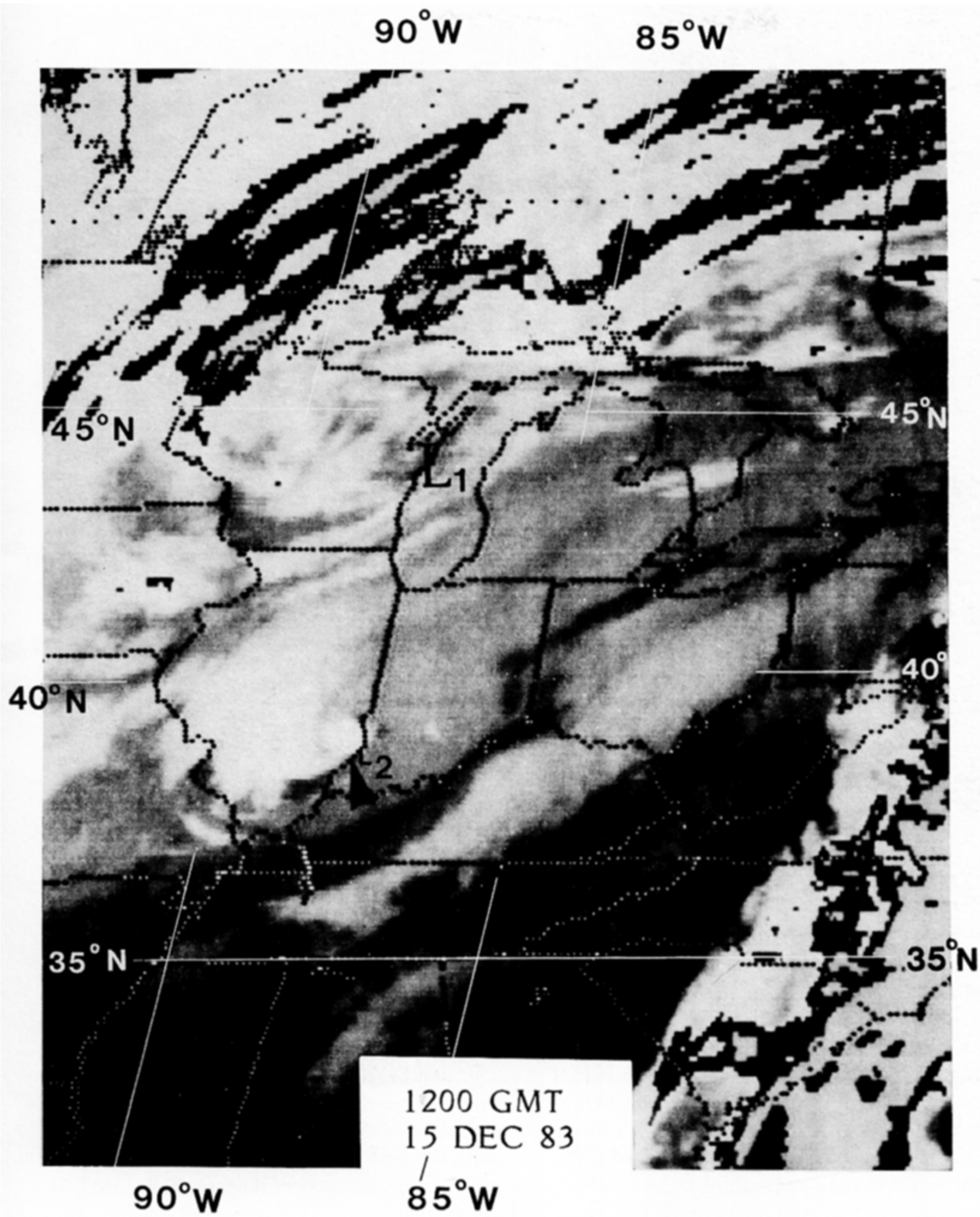

Fig. 7. 1200 GMT 15 December 1983 GOES IR satellite image. In this and the following figures, L_1 denotes the position of the surface synoptic low and the arrow points to the mesoscale low (L_2).

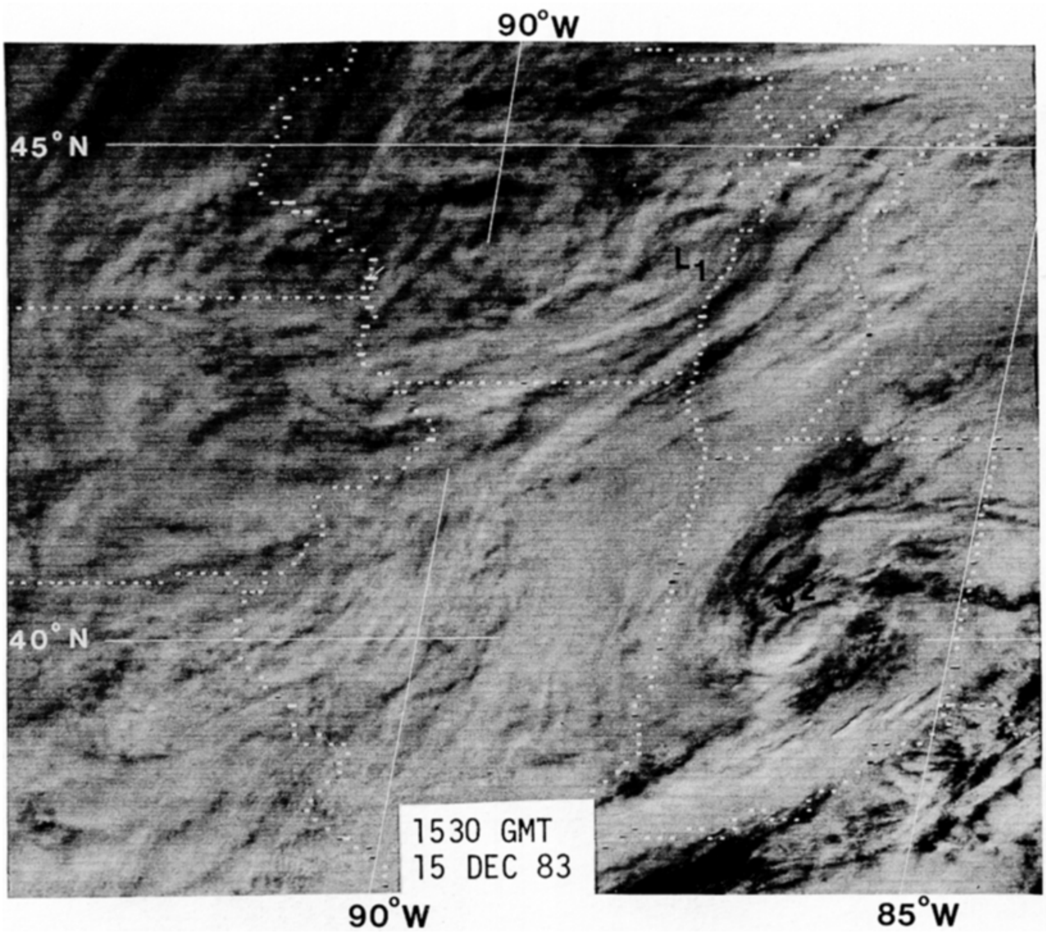

Fig. 8. 1530 GMT 15 December GOES visible satellite image showing the mesoscale low near Indianapolis, IN.

stationary front extended northeast into Canada. Fig. 11b shows the accompanying 700 mb contour analysis, which depicts a shortwave trough between Flint, Michigan (FNT) and Buffalo, New York (BUF). The 0000 GMT 16 December 1983 GOES IR image (not presented) showed the overcast in the Great Lakes and Ohio Valley regions, with two circulation centers evident. The one over Lake Michigan was the synoptic low and the one north of Lake Erie was the mesoscale vortex, which continued to show a spiral structure. By 1200 GMT 16 December the synoptic low had filled, leaving a weak cold frontal trough trailing from a 1004 mb low north of Maine, and the mesoscale vortex had dissipated.

3.2. Analysis

Other observational characteristics of this continental mesoscale vortex event are now described. Fig. 12 shows the path followed by the disturbance as it formed over Nebraska, propagated southeastward into southern Missouri, turned northeast passing over Salem, Illinois at the time of a sounding and finally dissipated in eastern Canada. This path is for the period 0000 GMT 14 December 1986 through 0930 GMT 16 January 1986.

While the mesoscale low never exerted a dominating influence at the surface (except for the heavy snow showers), it did affect the low and middle level cloud patterns. The satellite images revealed a generally elliptical region of

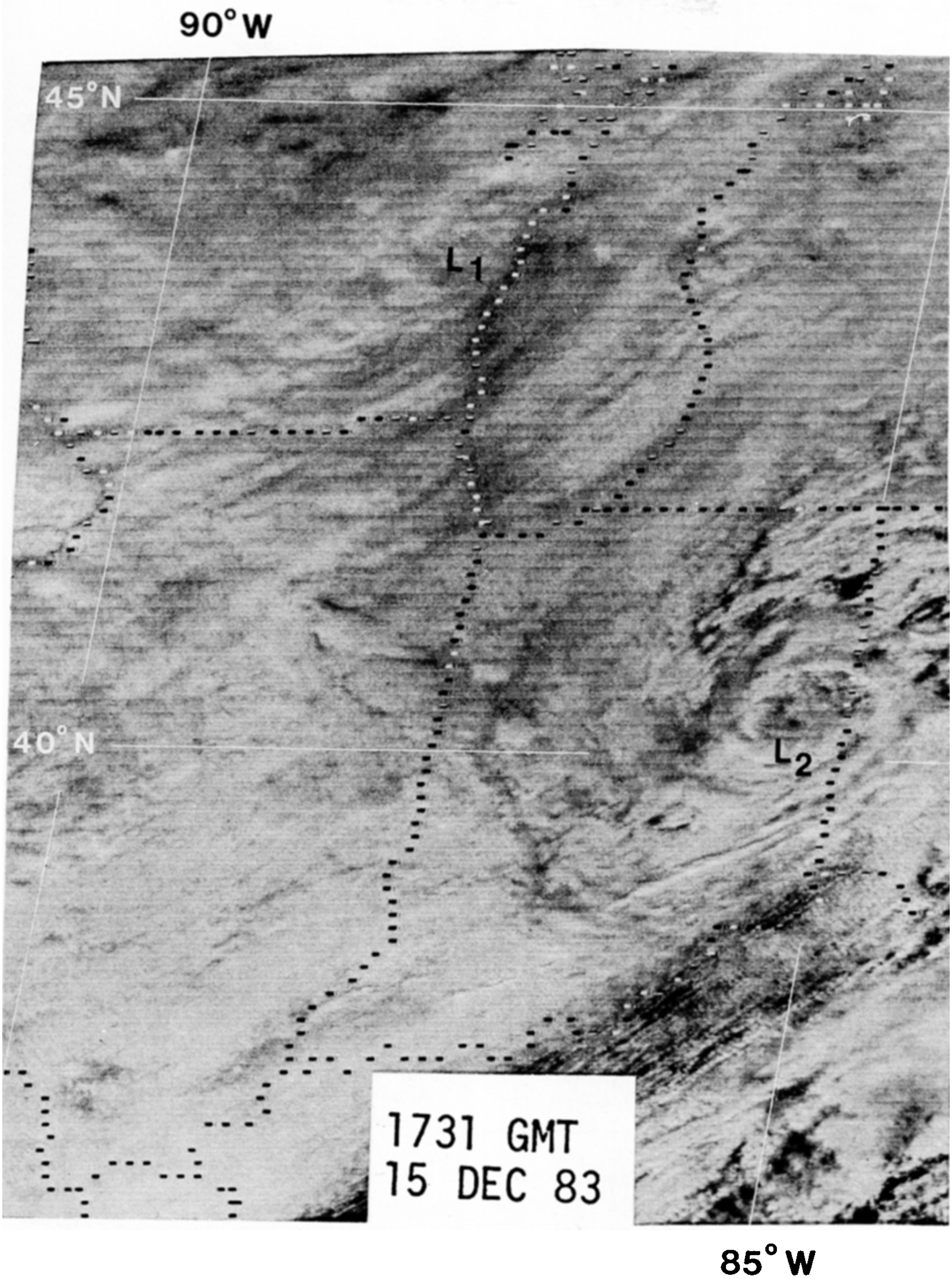

Fig. 9. 1731 GMT 15 December GOES visible satellite image showing the mesoscale vortex L_2 south of Ft. Wayne, IN.

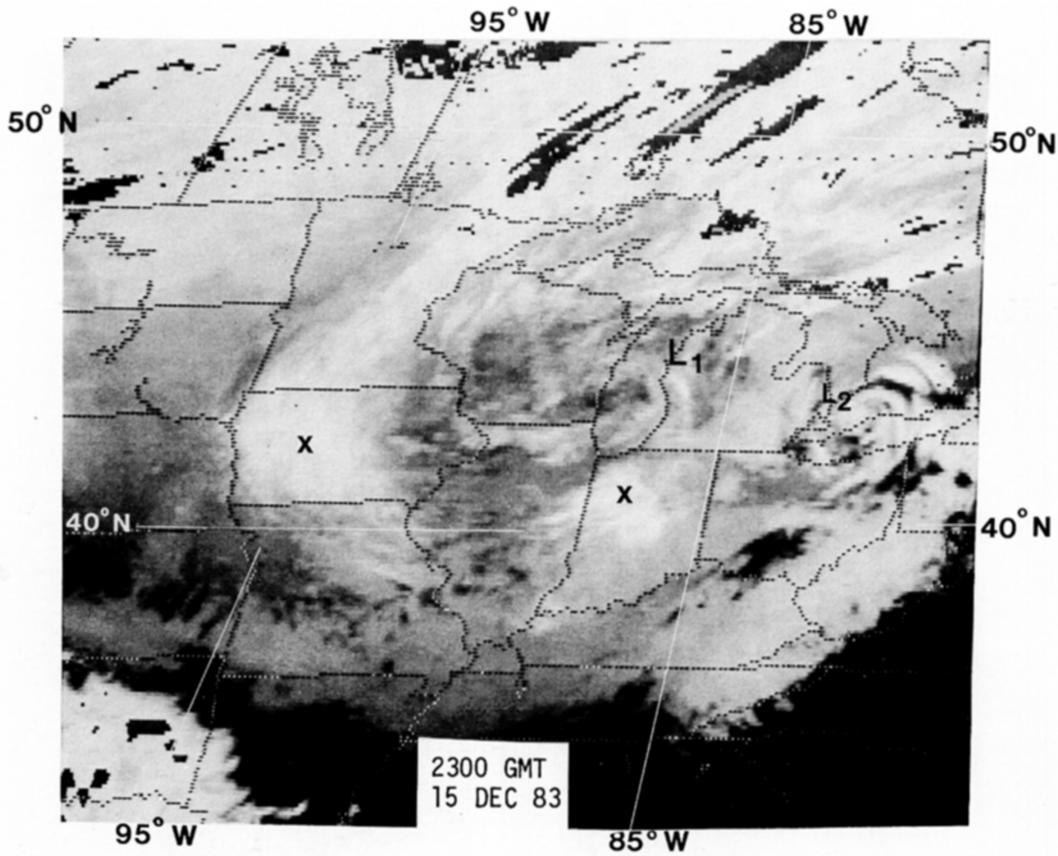

Fig. 10. 2300 GMT 15 December GOES IR satellite image showing the mesoscale low over Ontario, Canada. Note the two disturbances (denoted by x's) which appear to be trying to form as in a wavetrain with the mesoscale low L_2 as they all travel around the synoptic low, L_1.

influence which had a mean diameter ranging between 200 and 350 km. The diameter was calculated by averaging the longitudinal and transverse extents of the circulation pattern in the cloud images. In the upper air, this mesoscale event essentially slipped through the synoptic scale network (except over SLO), thus an accurate measurement of the disturbance wavelength was made difficult by the distances between stations. In an effort to define the size of this disturbance with more certainty, PROAMU analyses of the height fields were studied to find the wavelength in the upper levels. The best estimate of wavelength was obtained from the superposition of the short wave associated with the polar low on the synoptic height field at 1200 GMT 15 December (presented in the next section). The mesoscale low was associated with an analyzed wavelength disturbance of about 600 km.

Another interesting characteristic of this vortex event was its speed of movement. Fig. 13 shows that the mesoscale low moved at less than 5 m s^{-1} in the early stages, accelerating to about 10 m s^{-1} as it traveled to the southeast. Its speed increased to greater than 15 m s^{-1} as it turned to the northeast. As the vortex passed through Indiana, Ohio and into Canada, its speed increased further, traveling at more than 20 m s^{-1} between 1800 and 0000 GMT, 15 December,

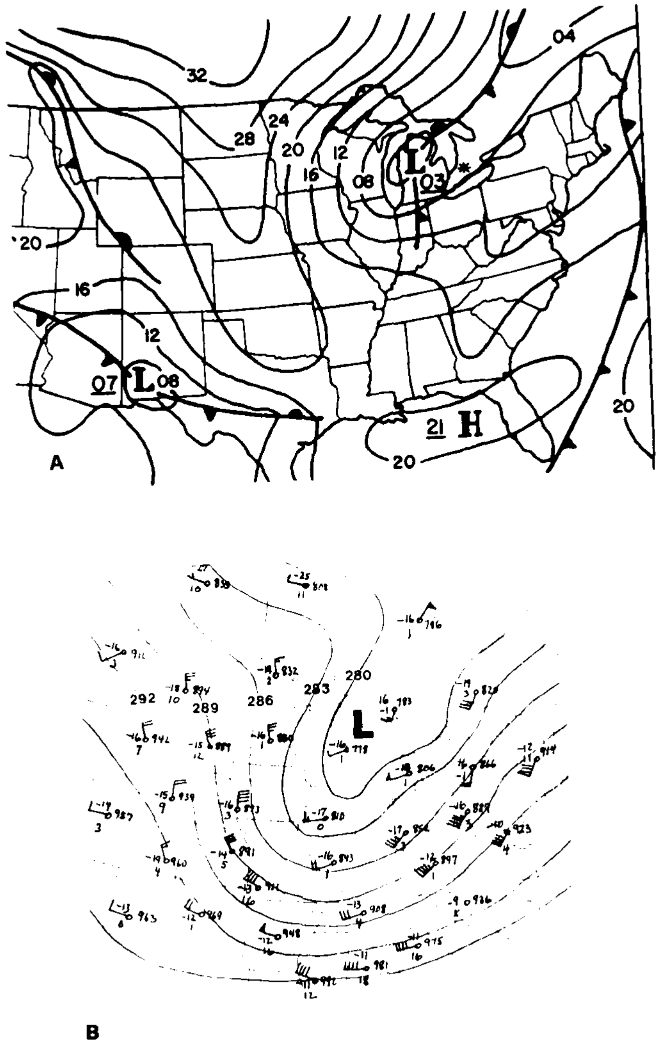

Fig. 11. (a) 0000 GMT 16 December surface analysis. (b) 0000 GMT 16 December 700 mb data and height field analysis, labeled in decameters.

slowing to about 15 m s^{-1} after that. The speed was estimated from three-hourly positions along the path.

Inspection of the surface pressure fields reveals the general synoptic pattern in the regions during the passage of the mesoscale low. There was no clear signal of the vortex at any of the three analysis times. This low never developed to the stage where the (total) surface pressure field was affected, contrary to the more intense Pacific and Atlantic cases. However, Rasmussen (1983) noted that the cloud patterns of some of the Barents Sea polar lows became quite well-developed in the satellite images well before the effects were felt in the surface analyses. The surface temperature analyses also showed a similar lack of a distinct signal. Again the vortex event was apparently not well developed enough to affect the surface-temperature field to the point where any mesoscale signal was present.

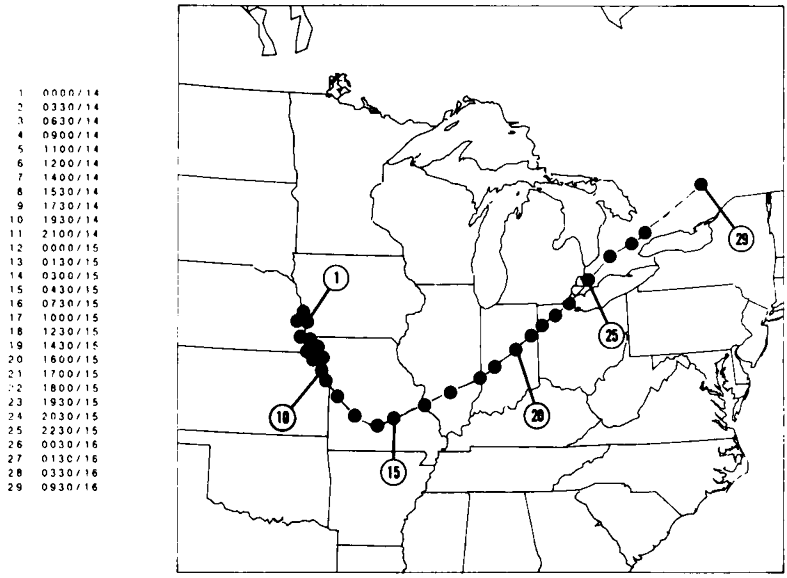

Fig. 12. Path followed by the mesoscale vortex between 0000 GMT 14 December and 0930 GMT 16 December 1983.

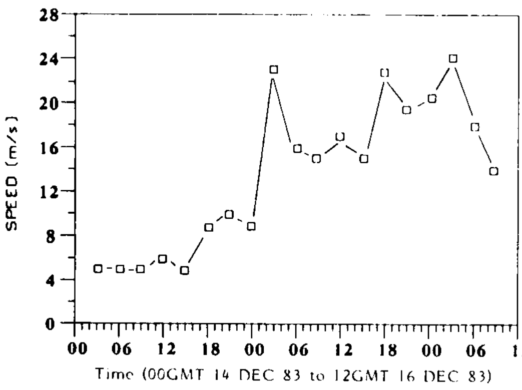

Fig. 13. Speed of the mesoscale vortex with time.

Independent hand analysis of the surface fields also supported the conclusions from the objective analysis methods. The moisture field had a lack of structure, similar to that of the temperature field. The wind field was dominated by the circulation around the synoptic low as it moved from west-central Indiana north into eastern Wisconsin. As with the other surface fields, the mesoscale low is not apparent in the wind field. Since vorticity and divergence values are derived from the wind fields, it was not surprising to find that conclusive patterns associated with the low did not appear at the surface. Based on these analyses, the mesoscale-vortex event was essentially invisible at the surface (however, analysis presented later will show a detectable mesoscale signal when the total fields are partitioned into synoptic and mesoscale components).

A number of lower tropospheric analyses were prepared to determine the structure and dynamics of this mesoscale vortex. Temperature, moisture, heights and winds were examined as well as the derivative fields obtained from these base quantities. The 700 mb analyses are presented and discussed, because the effects of the low were most pronounced at that level.

3.2.1. 700 mb level. Beginning with the height fields at 1200 GMT 14 December (Fig. 14a), the analysis shows a low center (2761 m) in southeastern Nebraska. Strong tilt in the synoptic system is evidenced by the surface position of the synoptic low in central Indiana at this time. The mesoscale low was centered in the extreme northwest corner of Missouri, as evident in the satellite images. Although the mesoscale vortex feature

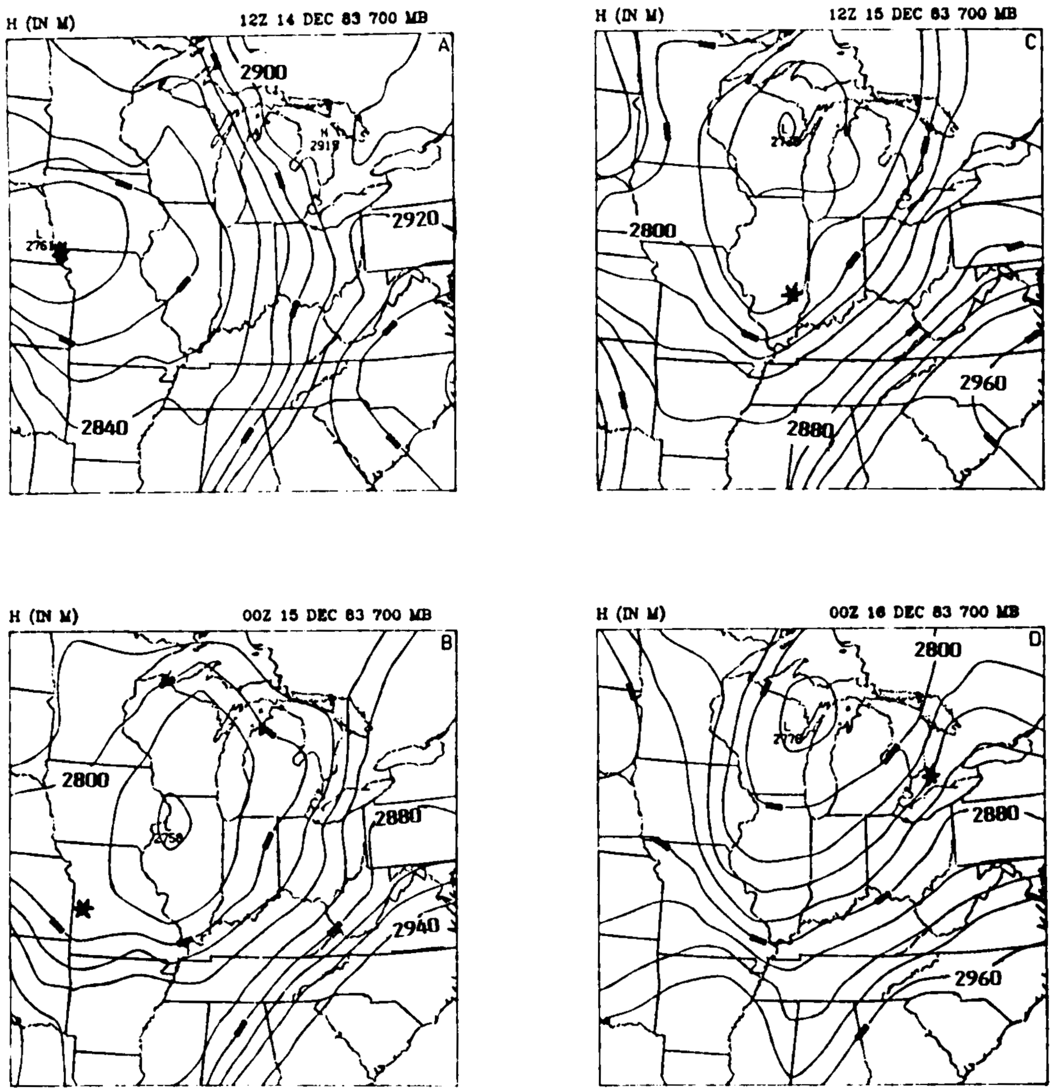

Fig. 14. 700 mb height field analyses for (a) 1200 GMT 14 December, (b) 0000 GMT 15 December, (c) 1200 GMT 15 December, and (d) 0000 GMT 16 December.

(denoted by *) now appears in the synoptic scale low (as already seen at the 500 mb level), the subsequent analysis shows that this vortex is distinctly different from the low that moves into northeast Wisconsin. By 0000 GMT 15 December (Fig. 14b) the surface synoptic low had moved northward to a position over Lake Michigan and the 700 mb height analysis showed a low center (2758 m) over northwestern Illinois, which had deepened slightly compared to 12 h earlier. A trough extended westward into Nebraska, with the mesoscale low located in west-central Missouri near the Kansas border. A weak short wave associated with the low was beginning to form on the synoptic pattern in a region of cyclonic shear (as noted earlier near OMA). The 1200 GMT 15 December analysis (Fig. 14c) shows that the low center had

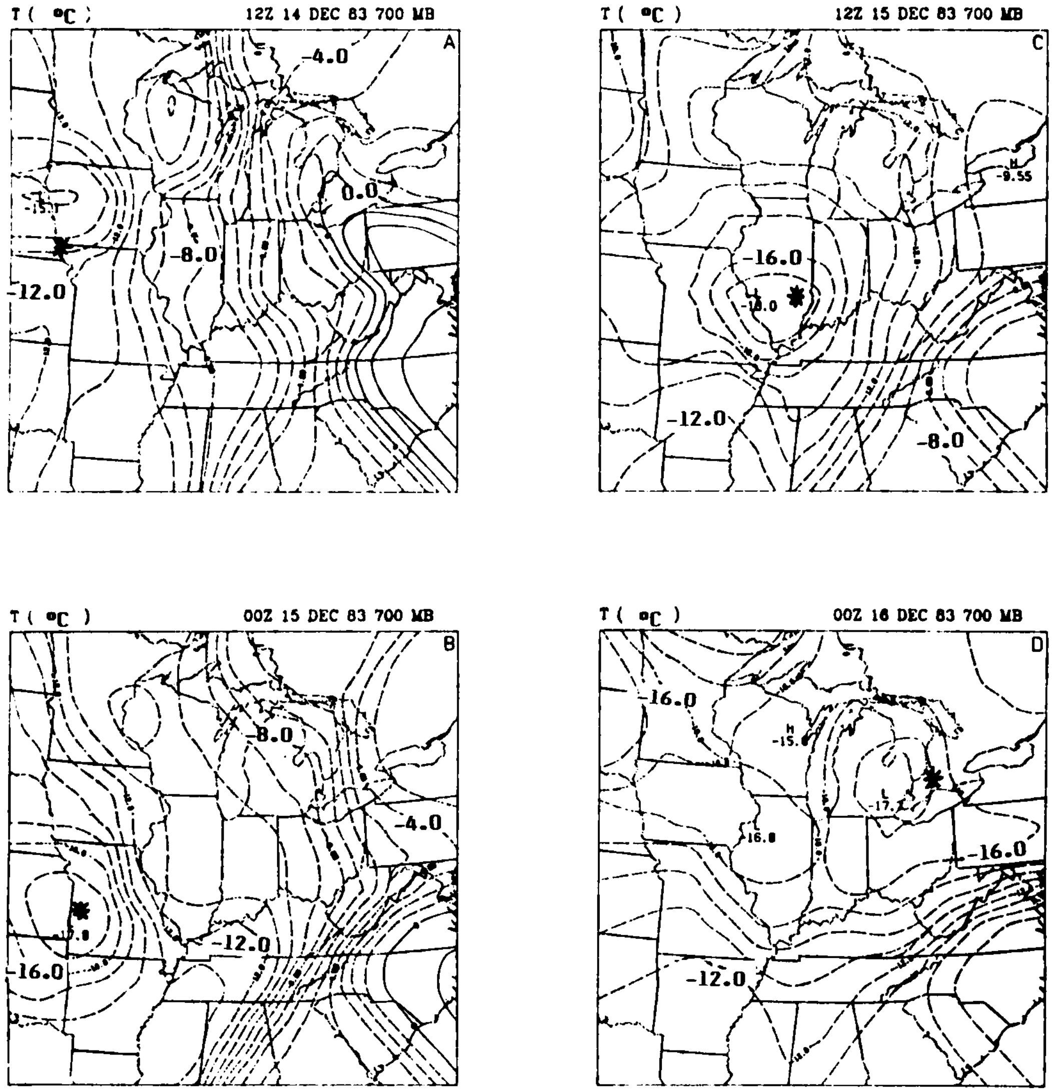

Fig. 15. 700 mb temperature analyses for (a) 1200 GMT 14 December, (b) 0000 GMT 15 December, (c) 1200 GMT 15 December, and (d) 0000 GMT 16 December.

deepened to 2738 m at 700 mb and had moved to northwest Wisconsin, while the surface synoptic low exhibited little movement and a 4 mb filling. The mesoscale vortex had moved into the cyclonic-shear zone and was located in southeast Illinois. The short wave had reached its maximum amplitude and exhibited a wavelength of approximately 600 km. This feature was captured objectively by the PROAMU analysis, and was not present in the NMC analysis. Also, the wavelength value (600 km) was consistent with size of the cloudy region (300 km) associated with the mesoscale vortex. The last upper-air observing time during which the mesoscale vortex existed was 0000 GMT 16 December. The height analysis (Fig. 14d) shows that the synoptic low center (2776 m) had begun to fill but was still located in northeastern Wisconsin. The surface low at this time moved into north central Michigan. The mesoscale low, located over Ontario between Lake Huron and Lake Erie, still faintly exhibited the short wave at 700 mb. It continued to move out of the strong cyclonic shear region, and into the edge of an area of anticyclonic curvature in the contours. The vortex dissipated soon afterwards.

The cold dome is quite apparent in the 700 mb level at all four time periods (Figs. 15a–d). At 1200 GMT 14 December, a −15.1°C minimum was located just north of the mesoscale low. At 0000 GMT 15 December the minimum had cooled to −17.8°C, following the low. By 1200 GMT 15 December the minimum reached −18.0°C and again corresponded to the satellite position of the vortex. And finally, by 0000 GMT 16 December the minimum warmed slightly to −17.7°C, and the temperature gradient of the entire domain had weakened considerably. These

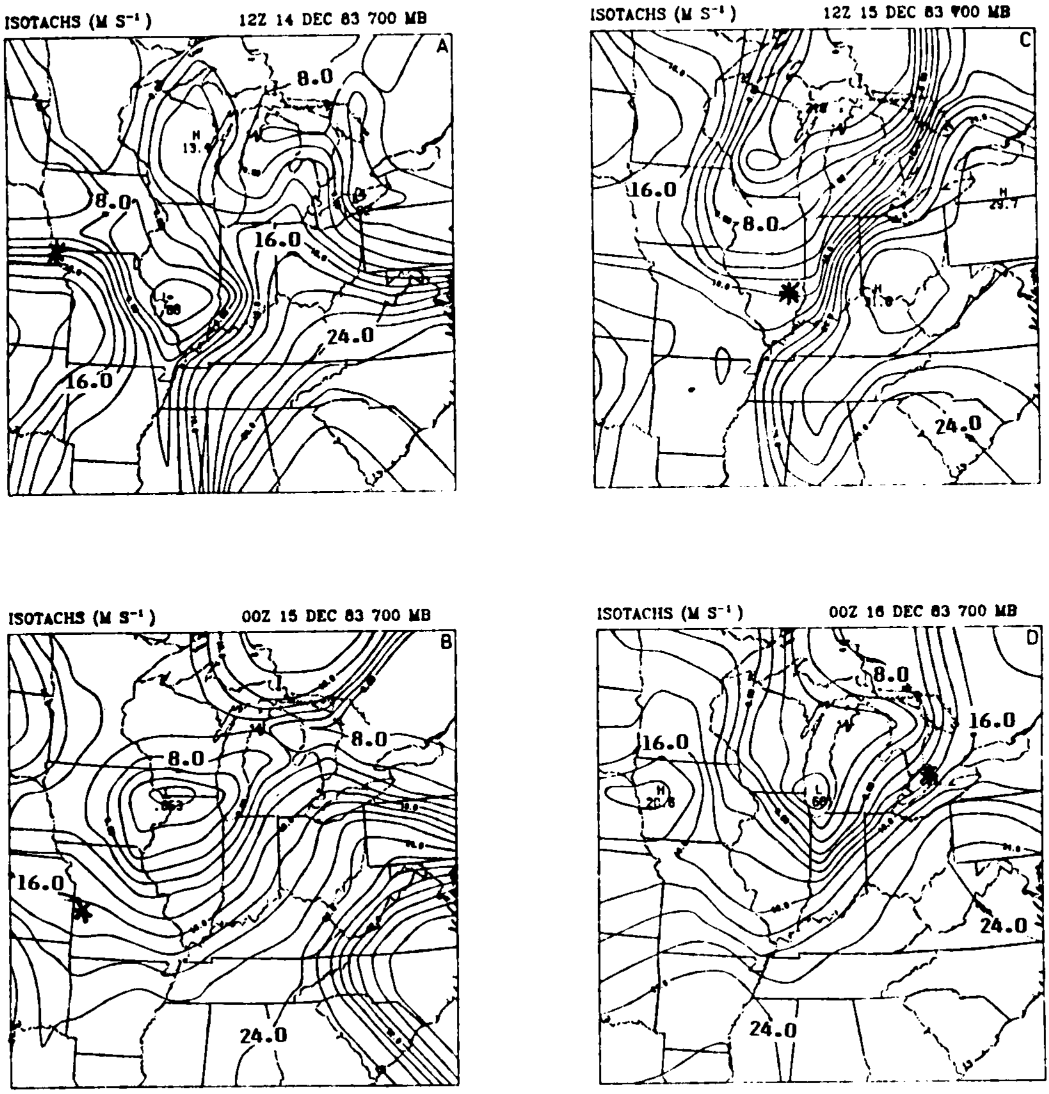

Fig. 16. 700 mb isotach analyses for (a) 1200 GMT 14 December, (b) 0000 GMT 15 December, (c) 1200 GMT 15 December, and (d) 0000 GMT 16 December.

analyses clearly show that the cold dome followed the mesoscale vortex, and not the synoptic scale feature to the north.

The wind field analyses show generally cyclonic large-scale flow centered more or less on the synoptic low. The isotachs (Figs. 16a–d) show large regions of strong cyclonic shear in the horizontal wind. Through all four time periods the mesoscale low exists in 700 mb cyclonic shear and, for the first three periods, in cyclonic curvature. The horizontal shear was approximately $4.0 \times 10^{-5}\ s^{-1}$ in the neighborhood of the low at all four time periods, but at 1200 GMT 15 December, the vortex was entering the region of central Indiana with nearly twice the shear ($7.5 \times 10^{-5}\ s^{-1}$). This region of increased shear was present at both 1200 GMT 15 December and 0000 GMT 16 December, indicating that the low passed through it between soundings.

3.2.2. Cross-sectional analysis. Cross-sections in both time and space and skew T–$\log p$ diagrams were plotted for several meteorological quantities. The time cross sections of virtual potential temperature (Θv) at SLO (Fig. 17) shows the vertical structure of the mesoscale low. With vortex passage directly over SLO during the 1200 GMT 15 December sounding, the cross-section shows the vertically stacked low-level warm core and "upper-level" (850–550 mb) capping cold dome. Strong destabilization in the Θv field and lowering of static stability is noted. The cloud areas were superimposed on the cross-section as indicated from the individual soundings (dewpoint depressions less than 3°C). A comparison with the spatial cross-section taken through the path of the low (Fig. 18) shows again the cold dome above about 900 mb. The low-level warm core is not evident in this cross-section, a condition which supports the surface observations and presence of a weak surface signal. This spatial cross-section provides evidence that this mesoscale vortex event is confined to the lower troposphere.

Further evidence of the destabilization caused by the mesoscale low is shown in Fig. 19. The 1200 GMT 15 December sounding was superimposed on the 0000 GMT 15 December sounding in a version of the before-and-after (more accurately, the before-and-during) effects of the vortex passage. Warming occurred between the surface and 830 mb and cooling above that to about 460 mb. The passage of the mesoscale low also caused the sounding to be saturated throughout the lower troposphere up to about 550 mb.

The mesoscale vortex had a similar structure earlier in its lifetime, even when less organized. At 0000 GMT 15 December, the disturbance was near Topeka, Kansas (TOP). Fig. 20 reveals the same cold dome over low-level warm core structure in the time cross-sections, though both are less pronounced. The same structure is evident in the Omaha, Nebraska (OMA) time cross-section (Fig. 21) at 1200 GMT 14 December when the

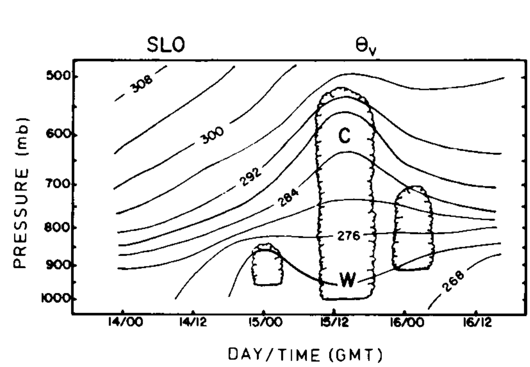

Fig. 17. Time cross-section of vertical distribution of virtual potential temperature at Salem, IL (SLO), 0000 GMT 14 December to 1200 GMT 16 December. W identifies the warm core at low levels, and C the strong capping cold dome.

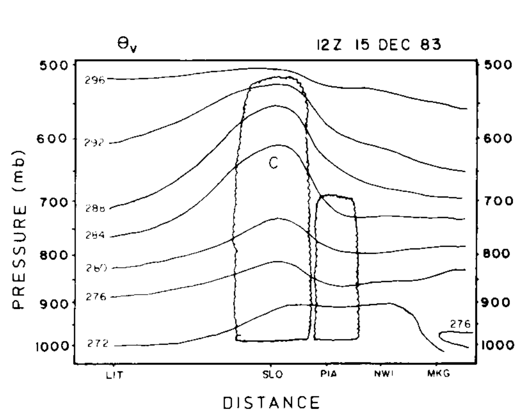

Fig. 18. Spatial cross-section of vertical distribution of virtual potential temperature across the path of the mesoscale low at 1200 GMT 15 December.

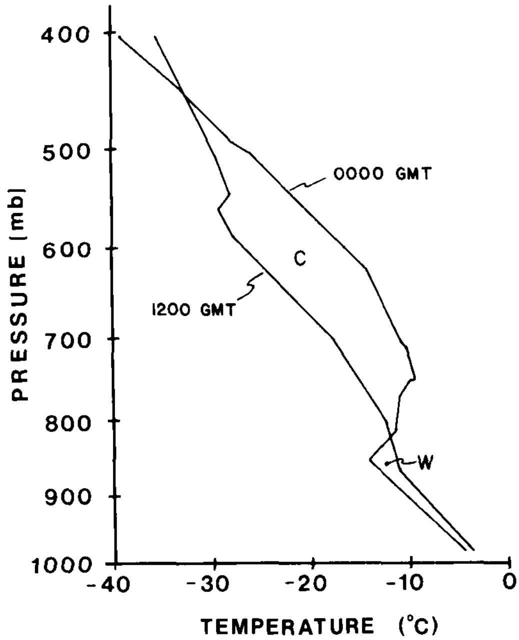

Fig. 19. Superposition of 1200 GMT sounding on the 0000 GMT sounding at Salem, Illinois (SLO) on 15 December 1983 using a Stuve diagram.

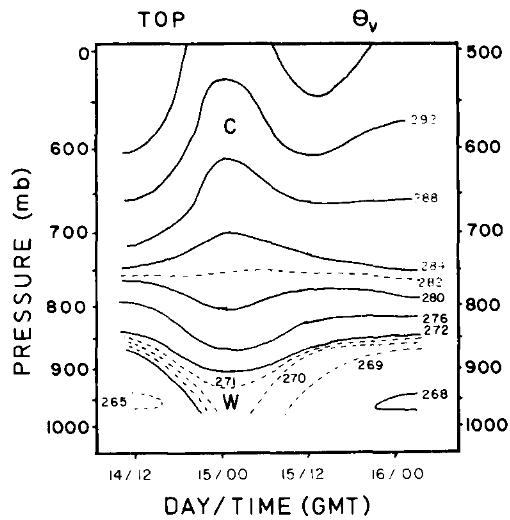

Fig. 20. Time cross-section of vertical distribution of virtual potential temperature at Topeka, Kansas (TOP), for 14–16 December 1983.

mesoscale low was little more than a swirl in the cloud pattern. Also, refer back to the 700 mb temperature field analyses presented in Figs. 15a–d, which clearly show the coincidence of the cold dome and the satellite derived position of the

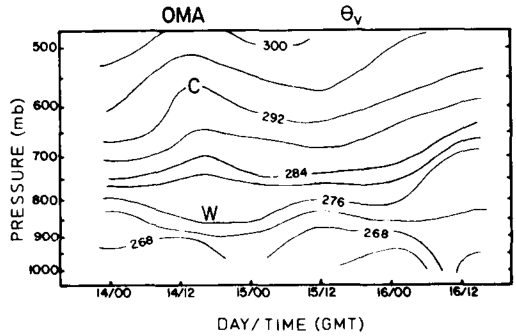

Fig. 21. Time cross-section of vertical distribution of virtual potential temperature at Omaha, Nebraska (OMA), for 14–16 December 1983.

mesoscale vortex. If one overlays the temperature patterns (Figs. 15a–d) and the height fields (Figs. 14a–d) the evolving baroclinic state can be observed, as the cold dome moves southeast out of the low center in the height field.

Unfortunately, the vortex event managed to avoid any other upper air stations after 1200 GMT 15 December. The small horizontal extent and position of the mesoscale low at 0000 GMT 16 December precluded any further analysis using the vertical cross-sections.

3.2.3. Mesoscale surface signal. At no time during the lifetime of this vortex did it dominate the surface weather (except for the associated heavy snow showers). Examination of the hourly surface observations and routine surface analyses revealed no sign of the mesoscale low. By looking in greater detail, however, and using special surface observation reports (which are sent at irregular time intervals as conditions change significantly) a weak signal of the polar low was found at the surface. As noted earlier, Rasmussen (1983) indicates that some of the Barents Sea polar lows become well-defined in satellite images, before effects are seen in the surface analysis.

It must be recognized that an observation taken at a reporting station is made up of the sum of several signals. The total signal, ϕ_{tot}, is composed of the synoptic, mesoscale and microscale portions (ϕ_{syn}, ϕ_{meso}, and ϕ_{micro}, respectively) of the weather surrounding the observing station. In addition, there is a potential error term due to measurement and/or human error. The equipment and observation procedures are designed to minimize the error term and the microscale

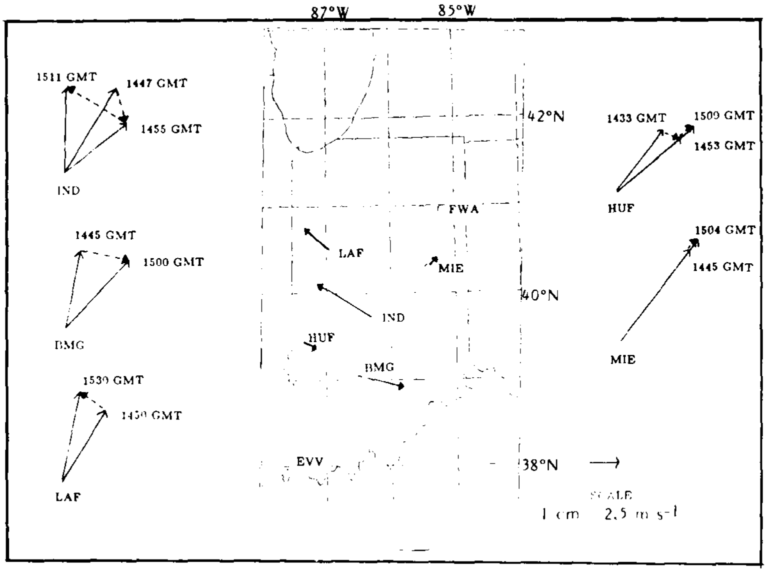

Fig. 22. Mesoscale wind fluctuations at ~1500 GMT 15 December due to influence of the polar low passage.

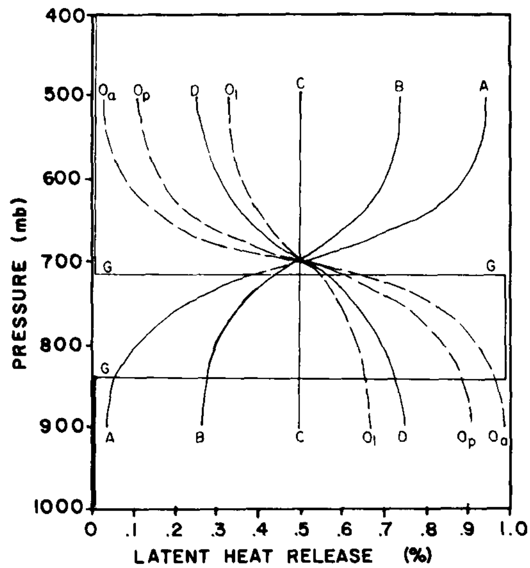

Fig. 23. Bratseth model CISK parameterization (Line G) superimposed on the Sardie and Warner model treatment of diabatic heating. Lines A–D represent modes in which the model was run for each of the case studies. The dashed lines represent observational case study data for five Atlantic, two Pacific, and this land case. See text for details.

fluctuations, but some does inevitably exist. Accordingly, the observations can be partitioned as:

$$\phi_{tot} = \phi_{syn} + \phi_{meso} + \phi_{micro} + \phi_{error}, \quad (1)$$

but the specified observing procedures effectively reduce the equation to:

$$\phi_{tot} = \phi_{syn} + \phi_{meso} + \phi_{error}. \quad (2)$$

Therefore, the mesoscale signal of the low can be retrieved from the surface reports by subtracting the synoptic signal from the total signal.

The application of this idea to the surface observations (including the specials) as the vortex crossed Indiana, is shown in Fig. 22. The biggest effect is seen in the wind field. The largest perturbation in the wind is approximately 3.5 m s^{-1}, which is the departure between the regular report (1455 GMT) and the special report (1511 GMT) at IND. The temperature field was not noticeably affected. The surface pressure varied about 0.7 mb, which is not much more than the range in instrument error. This weak surface signal occurred during a time when the mesoscale low was about as well developed as ever in its relatively short life.

3.3. Model applications

The Bratseth (1985) model treatment of pure CISK and the Sardie and Warner (1983) model treatment of moist baroclinicity and CISK (previously defined as SW) are now considered. Fig. 23 shows the Bratseth model heating parameterization superimposed on the SW model treatment of diabatic heating. Line A indicates the SW CISK parameterization with 90% of the latent heat being released in the upper layer (600 mb) and only 10% released in the lower layer (800 mb). Lines B–D represent increasing amounts of moist baroclinicity (in 25% increments) mixed with CISK, and Line O_p is an average of the Pacific Ocean polar-low case studies presented in SW and represents moist baroclinicity with CISK (83.5% of the latent heat released in the lower layer and 16.5% in the upper layer). Line O_a is an average of the five SW Atlantic Ocean case studies and represents a release of 93% of the latent heat in the lower layer and 7% in the upper layer. Line G represents the Bratseth parameterization of latent heat release, and Line O_l represents moist baroclinicity with CISK based on results from the 14–16 December continental case study. Line G was based on an isolated box-shaped heat source with $H1 = 500$ m and $H2 = 2500$ m (see Bratseth, 1985). Line O_l was calculated using values of this case study substituted into eqs. (4a–c) of SW. The data for Lines O_p, O_a and O_l are summarized in Table 1. The curves presented (except Line G) are based on two calculated points (at 600 and 800 mb) and a proposed cubic equation for smooth vertical redistribution of latent heat release. Line G is presented in a box-like fashion, analogous to a switch turned on or off (for a layer).

Table 1 is adapted from SW and includes the 1200 GMT 15 December sounding from SLO for comparison with the other seven cases. In addition, the values from the Peoria, IL (PIA) and Monett, MO (UMN) soundings from the same time are included as proximity soundings for comparison since the seven oceanic cases from SW were not favored with soundings through the centers of the polar lows. Some interesting similarities and differences were revealed.

Table 1. *Model parameters based on seven case studies of polar lows from Sardie and Warner (1983) and the 1200 GMT 15 December soundings for Salem (SLO), Peoria (PIA), and Monett (UMN)*

		Atlantic					Pacific		1200 GMT 15 December		
Param	Units	NNS	LKI	LKII	OTT	RAS	MUL	HOB	SLO	PIA	UMN
Length	km ± 100	700.0	700.0	600.0	1100.0	900.0	−1500.0	1500.0	−600.0	−600.0	−600.0
G-Rate	10^{-5}	3.3	2.0	2.0	3.2	1.85	—	−1.2	N/A	N/A	N/A
Lat	°N	65.0	55.0	55.0	52.0	65.0	40.0	40.0	41.0	41.0	41.0
U_5–U_7	m s^{-1}	10.0	5.1	2.6	7.7	0.0	13.0	10.0	−9.0	−14.0	−8.0
U_7–U_9	m s^{-1}	10.0	5.1	−5.1	10.3	4.5	11.0	5.0	7.0	0.0	16.0
σ_6	$\times 10^{-6}$	1.0	1.5	1.5	−5.1	1.0	1.7	1.8	2.9	2.4	2.4
σ_8	$\times 10^{-6}$	0.46	0.82	0.64	0.81	0.65	0.91	1.2	1.8	2.3	4.0
Ri_6		4.0	23.0	22.7	5.04	—	4.01	7.3	14.25	4.98	15.0
Ri_8		1.9	12.39	4.26	3.05	—	3.02	18.6	14.69	—	6.25
η_6		1.31	0.91	0.93	1.65	1.66	0.98	2.22	0.53	0.66	0.68
η_8		2.09	1.25	1.62	1.13	1.94	1.34	2.59	0.66	0.71	0.40
R_{6b}		0.07	0.08	0.07	0.08	0.06	0.17	0.14	0.36	0.47	0.73
R_{8b}		0.93	0.92	0.93	0.92	0.94	0.84	0.86	0.64	0.53	0.27
R_{6c}		0.90	0.90	0.90	0.90	0.90	0.90	0.90	0.90	0.90	0.90
R_{8c}		0.10	0.10	0.10	0.10	0.10	0.10	0.10	0.10	0.10	0.10
q_{s5}	g kg^{-1}	0.02	0.04	0.03	0.02	0.03	0.12	0.30	0.65	0.66	0.86
q_{s6}	g kg^{-1}	0.10	0.12	0.12	0.09	0.14	0.52	0.90	0.74	1.17	1.79
q_{s7}	g kg^{-1}	0.33	0.38	0.33	0.33	0.38	1.01	2.19	1.35	1.62	2.20
q_{s8}	g kg^{-1}	1.01	0.88	1.01	0.59	1.15	2.46	3.15	1.83	3.33	3.15
q_{s9}	g kg^{-1}	2.19	1.93	1.93	1.71	2.19	4.51	8.00	2.20	2.63	2.08
q_b	g kg^{-1}	4.31	4.56	4.56	4.06	5.58	5.46	3.50	2.60	2.71	2.69
q_{s10}	g kg^{-1}	6.42	7.19	7.19	6.42	8.98	6.42	8.97	3.00	2.80	2.69

The numerical subscripts refer to the pressure level at which the parameter is valid. The parameters are as follows: wavelength, growth rate, mean latitude, upper and lower level wind shear, static stabilities, Richardson numbers, amount of latent heat available, fraction of heat released in the upper and lower layers for baroclinic and CISK processes, and saturation specific humidities (adapted from Sardie and Warner, 1983).

Table 2. *Values of the parameters used for calculation of growth rates from Bratseth model for this case study*

	1200 GMT SLO	0000 GMT SLO	Std. atms.	Bratseth
γ	0.5	0.5	0.5	0.5
H_1	100.0 m	1138.0 m	0.0 m	500.0 m
H_2	1290.0 m	2067.0 m	5586.0 m	1500.0 m
N	0.0093	0.0142	0.0110	0.0070

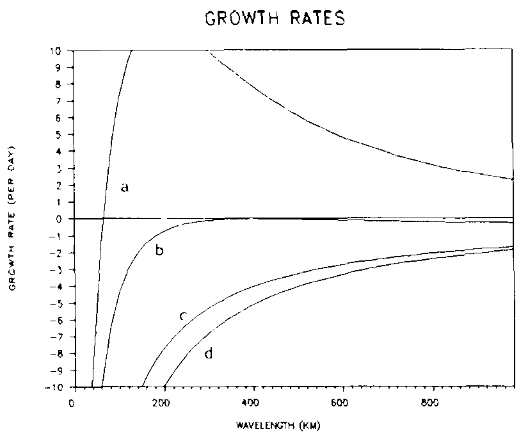

Fig. 24. Growth rate curves for (a) Bratseth's run, (b) 1200 GMT 15 December, (c) the Standard Atmosphere, and (d) 0000 GMT 15 December.

The 14–16 December land-based mesoscale low existed at an average latitude of 40° N, similar to the two Pacific polar lows and far south of the five Atlantic cases. The 900–700 mb shear was positive and comparable for all the cases, except for one Atlantic case which had negative shear in that layer. This case, however, characterized by negative shear in the 700–500 mb layer while the other seven cases continued to exhibit positive shear in that layer. This feature may have been a factor that contributed to the small development rate of the land case. The 600 and 800 mb static stabilities for the land case were larger by a factor of almost two, again contributing adversely to the growth rate of the low. The 600 and 800 mb Richardson numbers varied widely for the seven cases and the SLO values were somewhere in the middle. The total amount of heat available within the layers was given by η (see SW) and ranged between 0.91 and 2.22 in the upper layer and 1.13 and 2.59 in the lower layer.

The SLO calculations yielded values for η that were about half the lower limits of the oceanic cases. This was due mainly to the lower boundary layer moisture, q_b, in the land case, even though the 700–500 mb layer contained more moisture than the oceanic cases. This fact is reflected in the heating distributions, r_{6b} and r_{8b}, which were calculated from eqs. (4a–c) of SW. The five Atlantic cases exhibited baroclinic heat releases of 6–8% in the upper layer and the Pacific cases showed 14 and 17% heat release in the upper layer. The SLO calculations revealed 36% of the latent heat release in the upper layer, and from Fig. 23, Line O_1 indicates the possibility that more energy may be feeding the CISK-mode.

Although Bratseth did not use actual case study data, the values he used for the parameters were chosen to represent a very cold air mass of low stability over an ice-free ocean. The values for SLO were calculated from the 1200 GMT 15 December sounding.

A height of 100 m was used as the base of the heating layer, H_1, and the 850 mb level was used as the top for a layer thickness of 1190 m. The stabic stability, N (calculated from the Brunt–Väisälä formula) was 9.3×10^{-3} s^{-1} which is somewhat larger than the value of 7.0×10^{-3} s^{-1} used by Bratseth. The correction factor, γ, was set to 0.5 to adjust for the adiabatic nature of sinking motions. The rest of the values used are given in Table 2. The results of this run are compared with runs using the standard atmosphere and the SLO sounding from 0000 GMT 15 December (12 h earlier) all presented in Fig. 24. It is evident that the continental mesoscale vortex would not be expected to develop into a vortex as intense as the Norwegian Sea polar low, but some disturbances in the 300 km to 700 km wavelength range are nearly neutral (and may exist weakly for a few days).

Comparisons of this case with the seven SW case studies shows that this continental low exhibits characteristics of both Pacific and Atlantic polar lows. The shorter wavelength of this land-based event is more typical of the Atlantic polar lows. The Pacific events were characterized by greater amounts of moisture aloft than the Atlantic cases. This case exhibited even greater moisture aloft and is therefore more like the Pacific cases than the Atlantic cases. The heating distributions showed that this case is characterized by a much greater percentage of heat released in the upper level than the oceanic cases. The Bratseth model has shown that the growth rate of this case is not expected to be significant, though it should not decay rapidly, either.

4. Summary and conclusions

This paper has focused on a polar low case study, including both theory and observational results. A case study of a continental mesoscale vortex (in the interior of a polar air mass) has been analyzed and compared with model results. An attempt is made to incorporate these results into a more consolidated view of such vortex events (including their definition, phenomenology, structure and causative mechanisms).

A review of the literature on polar lows revealed a controversy centered on the instability mechanism responsible for their formation and development. One school of thought holds that polar lows are deep baroclinic phenomena such as those that commonly produce the Pacific comma cloud, although these systems can take other forms and even occur over land. The other school contends that polar lows are basically thermal instabilities driven by a CISK mechanism and as such, take on a highly convective spiral structure in the cloud pattern such as is often found in the North Atlantic. This type of polar low is generally not observed over land and in fact is often observed to dissipate rapidly upon land-fall. Some researchers previously felt that the comma cloud polar low and the spiral-form polar low were separate phenomena. Recent work, however, has led to the opinion that the difference is due to the proportions of baroclinicity and convective activity (in the form of CISK). It is also noted that barotropic instability may play a contributing role in some polar low events.

The continental case study event presented here formed near Omaha, Nebraska in mid-December 1983, and eventually dissipated in Ontario, Canada. This mesoscale low was unusual in that it occurred entirely over land, yet it exhibited many characteristics of oceanic polar lows. It was limited to the lower troposphere and the cloud tops were frequently only as high as the 600 mb level. It was not associated with any fronts and a well-developed cloud pattern was evident in the satellite imagery. The mesoscale vortex (and two subsequent lower tropospheric disturbances) rotated cyclonically around the south side of an existing occluded synoptic scale low (from the surface to the 500 mb level). Even though no distinct surface feature was evident, a weak mesoscale signal was found in a temporal analysis of the surface data. The vortex developed in an evolving baroclinic atmosphere, but also in the presence of strong cyclonic horizontal wind shear (a necessary condition for barotropic instability). It showed little to no tilt with height and had a weak low-level warm core capped by a strong cold dome maximized at the 700 mb level. It exhibited a comma-shaped structure early, which changed to a spiral structure (with an eye-like feature sometimes apparent) in the latter stages.

Two analytical models were used and results obtained to compare with the case study. It was found that the pure CISK model results by Bratseth (1985) and the combined moist baroclinicity and CISK studies by Sardie and Warner (1983) were consistent with the observed features of this vortex event and proposed causative mechanisms. It is further noted that Sardie and Warner (1985) modeled numerically the Rasmussen (1985) and the Locatelli et al. (1982) case studies, and concluded that both moist baroclinicity and CISK are essential for the genesis of polar lows. The results of the model comparisons made in this study with the 14–16 December 1983 case showed that it also had characteristics typical of both the Atlantic and the Pacific polar lows. The short wavelength and spiral structure of the cloud pattern was typical of the Atlantic polar lows. The latitude at which it occurred and the greater moisture aloft were, however, more typical of the Pacific polar lows. The large percentage of heat released in the upper level (compared to the lower level) lends credence to the importance of the CISK mechanism even in the development of a continental event. The Bratseth model growth rate calculation yielded a neutral growth rate which was consistent with observation. Also, the observational results reported here are consistent with the numerical model results by Orlanski (1986), in the manner that meso-baroclinic waves are affected by both static stability and the latent heat release.

Finally, this study suggests a possibly broader definition of the polar low event. Accordingly, it is defined as a lower tropospheric mesoscale vortex, which can occur over a land or water surface and within the polar air mass (thus removed from the polar front). The polar low often occurs within a cyclonic shear zone, satisfying the necessary condition for barotropic instability, and is uniquely characterized by a low-level warm core capped by a strong cold dome. Continental events may tend to be weaker and more shallow events than the oceanic lows, which tend to have strong synoptic features at the 500 mb level (Businger, 1987). The thermodynamic feature is viewed as a major finding in the observational part of this study, and one that future polar low modeling efforts must properly consider. It is further suggested that both barotropic and baroclinic instability mechanisms (combined with CISK) can exist cooperatively in support of the development and maintenance of both continental and maritime polar low events.

5. Acknowledgements

This work wsa supported by the NSF under the Experimental Meteorology Program Grant ATM-8505477 and Grant ATM-8711611, and by the DOD-Office of Naval Research, Marine Meteorology Program, under Grant N00014-86-K-0179. The authors would like to thank Dan Vietor for computer programming assistance; Deirdre Kann, Steve Vavrus and Carla Breiner for preparations of the figures; and Barbara Gilkes for manuscript preparation.

REFERENCES

Bratseth, A. M. 1985. A note on CISK in polar air masses. *Tellus 37A*, 403–406.

Businger, S. 1985. The synoptic climatology of polar low outbreaks. *Tellus 37A*, 419–432.

Businger, S. 1987. The synoptic climatology of polar-low outbreaks over the Gulf of Alaska and the Bering Sea. *Tellus 39A*, 307-325.

Carleton, A. M. 1985a. Synoptic cryosphere–atmosphere interactions in the northern hemisphere from DMSP image analysis. *Int. J. Remote Sensing 6*, 239–261.

Carleton, A. M. 1985b. Satellite climatological aspects of the "polar low" and "instant occlusion". *Tellus 37A*, 433–450.

Duncan, C. N. 1977. A numerical investigation of polar lows. *Quart. J. Roy. Meteor. Soc. 103*, 255–268.

Gall, R. L. 1976. The effects of released latent heat in growing baroclinic waves. *J. Atmos. Sci. 33*, 1686–1701.

Harrold, T. W. and Browning, K. A. 1969. The polar low as a baroclinic disturbance. *Quart. J. Roy. Meteor. Soc. 95*, 710–723.

Locatelli, J. O., Hobbs, P. V. and Werth, J. A. 1982. Mesoscale structures of vortices in polar air streams. *Mon. Wea. Rev. 110*, 1417-1433.

Mansfield, D. A. 1974. Polar lows: The development of baroclinic disturbances in cold air outbreaks. *Quart. J. Roy. Meteor. Soc. 100*, 541-554.

Mullen, S. L. 1979. An investigation of small synoptic-scale cyclones in polar air streams. *Mon. Wea. Rev. 107*, 1636–1647.

Mullen, S. L. 1982. Cyclone development in polar air streams over the wintertime continent. *Mon. Wea. Rev. 110*, 1664-1676.

Nitta, T. and Yanai, M. 1969. A note on the barotropic instability of the tropical easterly current. *J. Meteor. Soc. Japan 47*, 127-130.

Orlanski, I. 1986. Localized baroclinicity: A source for meso-α cyclones. *JAS 43*, 2857–2885.

Rasmussen, E. 1979. The polar low as an extratropical CISK disturbance. *Quart. J. Roy. Meteor. Soc. 105*, 531-549.

Rasmussen, E. 1981. An investigation of a polar low with a spiral cloud structure. *J. Atmos. Sci. 38*, 1785–1792.

Rasmussen, E. 1983. A review of meso-scale disturbances in cold air masses. In: *Mesoscale meteorology—theories, observations and models* (eds. D. K. Lilly and T. Gal-Chen). Dordrecht, Holland: Reidel Publishing Co., 247–283.

Rasmussen, E. 1985. A case study of a polar low development over the Barents Sea. *Tellus 37A*, 407–418.

Reed, R. J. 1979. Cyclogenesis in polar air streams. *Mon. Wea. Rev. 107*, 38–52.

Sardie, J. M. and Warner, T. T. 1983. On the mechanism for development of polar lows. *J. Atmos. Sci. 40*, 869–881.

Sardie, J. M. and Warner, T. T. 1985. A numerical study of the development mechanisms of polar lows. *Tellus 37A*, 460–477.

Sheu, P. J. and Agee, E. M. 1977. Kinematic analysis and air–sea heat flux associated with mesoscale cellular convection during AMTEX 75. *J. Atmos. Sci. 34*, 793–801.

Smith, D. R. and Leslie, F. W. 1982. Evaluation of a Barnes-type objective analysis scheme for surface meteorological data. NASA Tech. Memo., *82509*, Marshall Space Flight Center, Huntsville, AL (USA), 25 pp.

Smith, D. R., Pumphry, M. E. and Snow, J. T. 1986. A comparison of errors in objectively analyzed fields for uniform and nonuniform station distributions. *J. Atmos. Oceanic Technol. 3*, 123–132.

Staley, D. O. and Gall, R. L. 1977. On the wavelength of maximum baroclinic instability. *J. Atmos. Sci. 34*, 1679–1688.